Fischer–Tropsch synthesis: changes in phase and activity during use

Nathila Sirimanothan [a], Hussein H. Hamdeh [b,*], Yongqing Zhang [a], and Burtron H. Davis [a]

[a] University of Kentucky, Center for Applied Energy Research, 2540 Research Park Drive, Lexington, KY 40511, USA
[b] Wichita State University, Physics Department, Box 32, Wichita, KS 67260, USA

Received 5 September 2001; accepted 8 May 2002

Four iron catalysts (unpromoted, K-promoted, Si-promoted and K,Si-promoted) were activated and subjected to common Fischer–Tropsch synthesis conditions. At increasing times on stream, samples were withdrawn from the continuously stirred tank reactor in the reactor wax while keeping the sample blanketed with an inert gas. Mössbauer spectra were recorded for various samples and the iron phases of the catalyst were compared to the catalytic activity. A simple model based on bulk composition of the catalyst is not related to the catalytic activity during the course of the run.

KEY WORDS: Fischer–Tropsch synthesis; iron catalyst; Mössbauer studies of iron.

1. Introduction

During use, iron-based Fischer–Tropsch synthesis (FTS) catalysts undergo two general types of deactivation. One deactivation pathway can be classified as physical degradation since the integrity of the catalyst particles is destroyed. This is a serious problem because it makes fine particles that cannot be easily separated from the heavy wax products, that will increase the viscosity of the slurry, that may cause extreme pressure drops, etc. This aspect of deactivation will not be considered here. The other deactivation pathway can be classified as being due to chemical or phase changes. With an iron catalyst, two forms are usually present under FT conditions: Fe_3O_4 and iron carbides. The chemical changes usually cause decreases in catalytic activity and/or alteration of the product selectivity.

Iron-based FT catalysts are employed in the industrial setting in either low (<573 K) or high (>593 K) temperature regimes. Because the major portion of the production at Sasol has been carried out with high-temperature catalysis and because of significant early operating problems due to catalyst deactivation, much of the current understanding of this subject has been developed from high-temperature studies. Several possible causes of catalyst deactivation have been postulated for the high-temperature operations: (i) sintering, (ii) carbon deposition and (iii) phase transformations [1]. With respect to phase transformations, there is considerable disagreement whether the active phase for FTS is iron oxide or carbide [2,3]. In addition, certain reactor conditions, such as a high partial pressure of water, are known to cause a decline in activity [4].

* To whom correspondence should be addressed.

It is well established that iron-based FTS catalysts undergo a series of phase transformations during activation and use [1]. Activation with carbon monoxide or syngas typically results in the conversion of Fe_2O_3 to Fe_3O_4 and ultimately to one or more carbides [5]. During FTS, iron carbides can be oxidized to Fe_3O_4 if the H_2O/H_2 or CO_2/CO ratios are high enough [1]. As indicated above, there has been considerable debate about the active phase of FTS. Some studies have indicated that FTS requires an active oxide species [2] while most have supported a carbide species [5,6].

Mössbauer spectroscopy has proven to be an effective technique for the analysis of iron-based FT catalysts. *In situ* Mössbauer studies have been reported [3,7]; however, these studies have been performed at low pressure and low conversions. Studies performed at industrially relevant conditions have generally involved removing the catalyst from the reactor followed by passivation [8] which, if not performed properly, will oxidize the catalyst [6].

The early works directed toward defining the role of different carbide species that are present during CO hydrogenation have been reviewed [9]. It has been suggested that ε- and ε'-carbide (Fe_2C and $Fe_{2.2}C$, respectively) are responsible for catalysis following CO dissociation [10,11]. Hägg carbide formation has been considered to decrease the activity of the catalyst [3]. On the other hand, it has been claimed that the deactivation of iron catalysts in FT synthesis is associated with the transformation of high-activity Hägg carbide to less active ε-carbides and to the formation of a highly-ordered graphite on the surface of the catalyst [12].

Tau *et al.* [13] utilized an *in-situ* Mössbauer cell to follow changes in 10% Fe–Al_2O_3 (Alon-C) and 10% Fe–SiO_2 (Cab-O-Sil) catalysts. Using the nomenclature of Niemantsverdriet [14], the progressive carburization in

1011-372X/02/1000-0181/0

10% CO/H_2 at 558 K, following reduction in H_2 at 723 K, produced the following progression: $Fe \rightarrow Fe_xC \rightarrow \kappa\text{-}Fe_{2.5}C \rightarrow \varepsilon'\text{-}Fe_{2.2}C$. The authors cautioned that this sequence was not followed for an unsupported iron catalyst [14] nor even for a supported catalyst that was similar to the one they used [15]. Their composition was not consistent with the usual order of stability of the carbides where the ε'-$Fe_{2.2}C$ form, when heated, loses carbon to form the κ-form and then the θ-form. After 30 min the bulk of the iron was about 74% carburized to a mixture of κ-$Fe_{2.5}C$ and ε'-$Fe_{2.2}C$ [16]. They reported that at longer synthesis times, the ε'-$Fe_{2.2}C$ form predominated.

Gatte and Phillips [17] evaluated the modeling routine used to obtain the iron phases from Mössbauer spectra and concluded that this is fraught with difficulties. In spite of this, they conclude that there is ample evidence to support the conclusion that at least one phase of octahedral carbide, normally called ε' carbide, forms during FTS; however, they cautioned that the spectra of ε'-carbide probably consists of at least two sextuples.

Deactivation studies of four catalysts (unpromoted iron, iron promoted with K, iron promoted with Si, and iron promoted with K and Si) that were activated and used under the same synthesis conditions showed initial (first 50 h) CO conversions that were essentially the same; however, as the run time increased beyond about 100 h the catalyst aged at different rates [18]. During the first 100 h of the run, the ratio of FTS rate and water–gas shift rate remained constant and had nearly the same ratio for the four catalysts. Thus, the common conversion level and essentially the same selectivity for water and CO_2 indicate that the four catalysts are exposed to similar gas-phase composition during the initial part of the run. Thus, the different aging rates should not be due primarily to the gas-phase composition.

Characterization data for catalyst samples withdrawn during the course of each run did not conform with any of the three reasons, based on the three changes advanced by Dry [1] that are given above, for catalyst deactivation. Herein are reported Mössbauer results obtained for four similar iron catalysts that were activated and used for synthesis in a slurry phase, continuously-stirred tank reactor (CSTR) at high initial conversion levels and under industrially relevant conditions. The conditions are the same as used in our previous report [18]. Strict measures were observed to prevent oxidation of the catalyst samples. The results reported here compare the iron phases present as these four iron catalysts are utilized at increasing reaction times for FTS.

2. Experimental

2.1. Catalysts

Catalysts were prepared by a procedure described previously [5,19]. Iron oxyhydroxide was precipitated from an aqueous solution of $Fe(NO_3)_3 \cdot 9H_2O$ (Johnson Matthey, 98+% metals basis, 1 M) at a feeding rate of 157 cm^3/min to a CSTR by adding a separate stream of concentrated NH_4OH (VW, reagent grade, 28–30 wt%) at 71 cm^3/min. The pH of the slurry was 9.3 and the residence time in the CSTR was 300 s. This operation produced a total slurry volume of 34.4 l. After the initial filtration, the filtrate was washed by re-slurring the filtrate in the amount of distilled de-ionized water required to bring the total volume of the re-slurried material back to 34.4 l for each of the two washings. Each of the filtrations utilized a rotary drum filter. The washed filter cake was dried in air at 373 K overnight. The dried catalyst was ground using mortar and pestle to particles of ~0.15 mm and then treated in stagnant dry air at 623 K for 4 h. A comparable potassium K-catalyst was obtained by impregnating the dried material with sufficient potassium nitrate solution to yield a finished catalyst with Fe : K atomic ratio of 100 : 0.71. A silicon (silica) promoted catalyst was prepared by the same procedure as outlined above for the unpromoted iron sample except that sufficient tetraethylorthosilicate was dissolved in the iron nitrate solution to provide a ratio of Fe : Si of 100 : 4.4 and the suspension was allowed to hydrolyze during three days prior to effecting the precipitation. A portion of the dried Fe : Si = 100 : 4.4 material was impregnated with sufficient potassium nitrate solution to yield a final catalyst with an atomic ratio of Fe : Si : K = 100 : 4.4 : 0.71.

2.2. Activation and FTS reaction

All FTS runs were conducted in a 1 L CSTR. The catalyst precursor (64.44 g) was suspended in C-30 oil (Ethylflow, a decene trimer obtained from the Ethyl Corp.; 290 g) and it was pretreated with CO at 543 K at 1.22 MPa for 24 h. The CO flow (58.7 SL/h g-Fe) was started at ambient conditions (298 K and 0.1 MPa), the pressure was raised to 1.22 MPa, and the reactor temperature was ramped to 543 K at 2 K/min and maintained at this temperature for 24 h. Following the activation treatment, the reactor was brought to reaction conditions, which were 543 K, 1.22 MPa , H_2/CO ratio of 0.68, and a total flow ($CO + H_2$) rate of 3.1 SL/h g-Fe.

Catalyst samples were removed at intervals from the autoclave during the reaction run using a dip tube blanketed with an inert gas. All subsequent handling of the used catalysts was carried out under an inert gas within a glove box. A total of 20 samples were withdrawn from the reactor during the 452 h run for the unpromoted sample and 17 samples during 400 h for the potassium-promoted catalyst. For the Si-promoted catalyst, a total of nine samples were taken during 215 h and for the Si,K-promoted catalyst a total of 13 samples were taken during 355 h.

Reaction products were analyzed using several chromatographs. Gas products were analyzed using a

Hewlett-Packard Quad-series refinery gas analyzer (QRGA) micro gas chromatograph. The analysis of the aqueous phase collected beyond the reactor used a Hewlett-Packard 5790 GC with a thermal conductivity detector and a Porapak Q column. Oil and wax samples were combined and analyzed with a Hewlett-Packard 5890 GC with a flame ionization detector and a 60 m DB-5 column. The reactor wax was analyzed on a Hewlett-Packard 5890 high temperature GC with a flame ionization detector and a 30 m alumina-clad HT-5 column.

2.3. Mössbauer spectroscopy measurement

The Mössbauer experiments used a constant-acceleration spectrometer. The radioactive source comprised 50–100 mCi of ^{57}Co in a Pd matrix. The samples in powdered form were loaded into Plexiglas compression holders presenting a thin sample to the beam. All spectra were analyzed by a least-squares fitting procedure, which attempts to describe the spectra as a series of Lorentzian peaks corresponding to the Mössbauer spectra of known Fe compounds. The fraction of the Fe atoms in each of the known phases is reported as the contributions of each of these known phases to the experimental spectrum.

3. Results

Table 1 contains Mössbauer data showing the unpromoted iron catalyst composition as a function of time-on-stream. Samples 1, 3, 10 and 20 are the used samples after activation and after various FTS times. The Fe_5C_2 phase was established from the measured hyperfine parameters, although the measured fraction ratio ($Fe_I : Fe_{II} : Fe_{III}$) did not conform to the expected ratio of 2:2:1. In large-crystal samples of the carbide, the ratio frequently differs from 2:2:1 due to the variable concentration of carbide carbon. Here, however, the deviation is more profound and indicates that crystallization is not complete. In spite of this, Fe_5C_2 is the only iron carbide that can be discerned from the Mössbauer measurements.

Table 1
Mössbauer structural analysis results for unpromoted iron sample

	Sample			
	1	2	3	4
FTS reaction time (h)	0	23	168	452
Fe_5C_3 (at%)	94	83	42	0
Fe_3O_4 (at%)	6	17	58	100

Catalyst samples for Mössbauer spectroscopy were withdrawn immediately after activation and at 23 h, 168 h and 452 h of FT synthesis. The distribution of iron in the catalyst after activation with carbon monoxide was 94% χ-Fe_5C_2 and 6% Fe_3O_4. Exposure to syngas initiated oxidation of the χ-Fe_5C_2 to Fe_3O_4. After 23 h of FT synthesis, 83% of the iron was present as χ-Fe_5C_2 and the balance was Fe_3O_4. The amount of iron present as χ-Fe_5C_2 had decreased to 42% after 168 h of FT synthesis. The only detectable phase after 453 h of FT synthesis was Fe_3O_4.

Syngas conversion and carbide-phase *versus* time-on-stream for the unpromoted iron catalyst are shown in figure 1. Syngas conversion after 24 h of FTS was

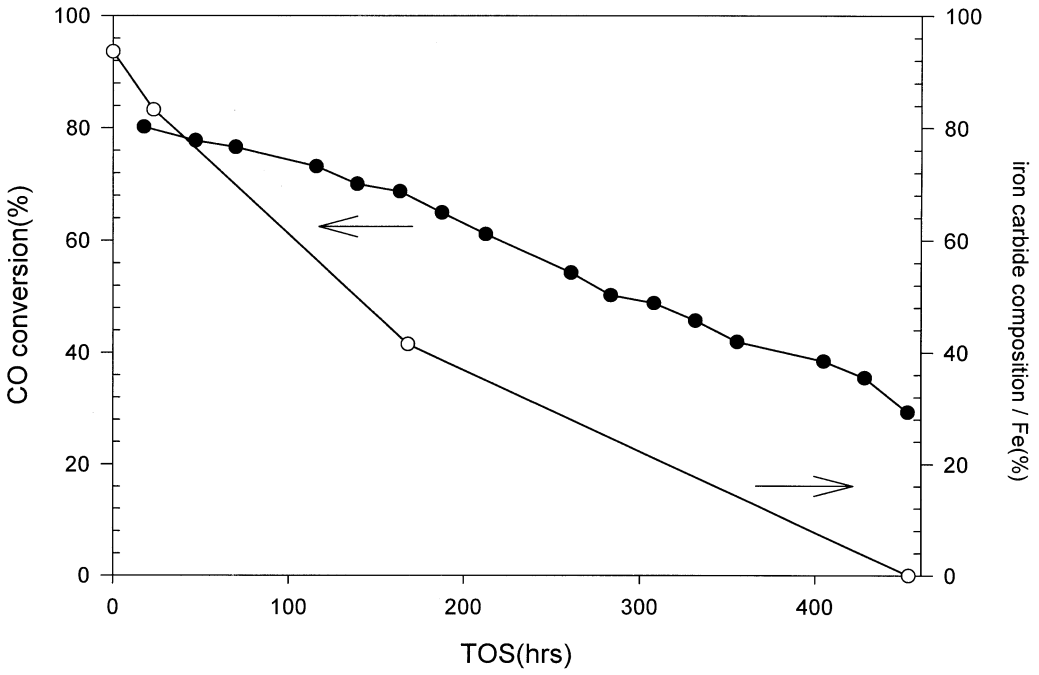

Figure 1. The changes in CO conversion (●) and total iron carbide phases (○) for a precipitated, unpromoted iron catalyst, activated in CO, during synthesis.

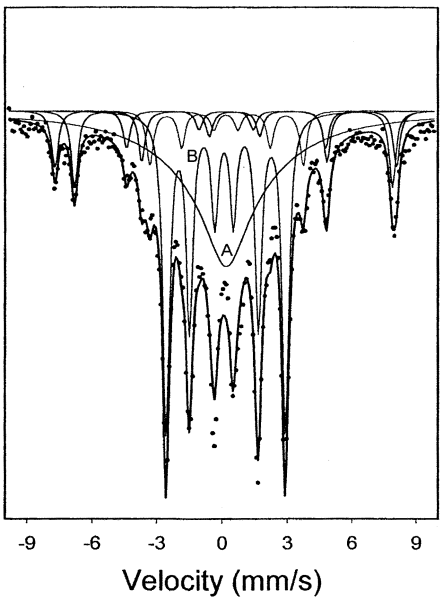

Figure 2. Mössbauer data (experimental points) and fitted spectra (A, superparamagnetic contribution, ε-Fe_2C) for a K-promoted iron catalyst after 48 h of synthesis time.

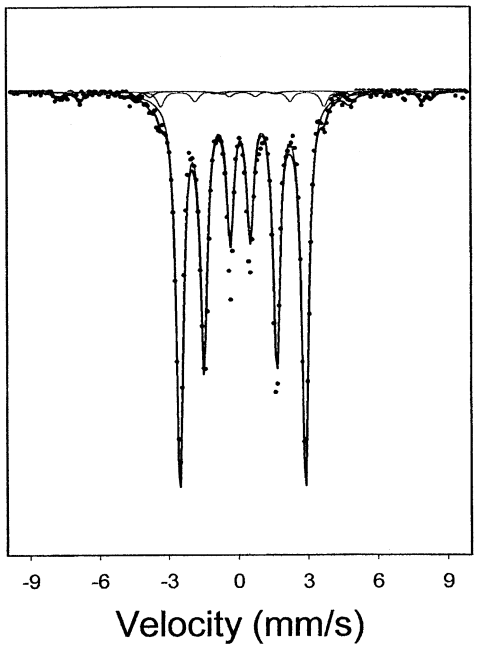

Figure 3. Mössbauer data (experimental points) and fitted spectra (see text for identification).

above 84% and is in excellent agreement with a similar catalyst whose results were reported earlier [18]. The catalyst activity declined steadily throughout the run with an average rate of deactivation of 0.16% h^{-1}; when the conversion is corrected for catalyst withdrawal the decline is slightly slower. The activity decline parallels the oxidation of the iron carbide to produce Fe_3O_4.

3.1. Potassium-promoted iron catalyst

The Mössbauer spectrum of the potassium-promoted sample taken at the earliest time-on-stream is more complex than the others in this series of catalyst samples and indicates that the sample contains 42 at% of superparamagnetic iron phase(s) (figure 2). The Mössbauer line widths are relatively sharp for the spectra recorded for the potassium-promoted samples that were withdrawn after about 100 h into the run (e.g., figure 3). The data for five samples are summarized in table 2. The data for sample 3 suggest that carbiding of the promoted iron catalyst is incomplete at the end of 24 h and continues during the early stages of the synthesis. However, after about 100 h on stream, the iron is present essentially as carbide phases. Thus, the latter four samples could be fitted to four sextets (sub-spectra), as shown by the deconvolution curves (figure 3). For sample 3, an additional collapsing spectrum, which originates from the superparamagnetic fine clusters, is necessary. It is reasonable to assign the major sextet (hyperfine magnetic field; HMF 168–170 kG) to ε-Fe_2C. The minor sextet (HMF 217–221 kG) is assigned to a phase with an excess of Fe and this phase may be designated as ε-$Fe_{2+}C$. The data obtained from low-temperature (20 K) measurements are similar to those obtained at room temperature (tables 2 and 3). This is not surprising since most of the samples were predominantly of the carbide form and the low-temperature

Table 2
Mössbauer structural analysis of spectra obtained at room temperature for potassium-promoted iron samples

Sample	Time-on-stream (h)	HMF [a]	Atomic aeral fraction (%)	Phase
3	48	491	6	A-site Fe_3O_4
		457	9	B-site Fe_3O_4
		219	6	$Fe_{2+}C$
		170	36	$Fe_{2+}C$
		Unknown	42	Superparamagnetic
5	97	490	3	A-site Fe_3O_4
		453	5	B-site Fe_3O_4
		228	6	$Fe_{2+}C$
		168	86	$Fe_{2+}C$
8	167	491	1	A-site Fe_3O_4
		457	2	B-site Fe_3O_4
		219	3	$Fe_{2+}C$
		170	93	$Fe_{2+}C$
11	259	493	2	A-site Fe_3O_4
		454	3	B-site Fe_3O_4
		217	2	$Fe_{2+}C$
		168	93	$Fe_{2+}C$
16	394	490	2	A-site Fe_3O_4
		453	2	B-site Fe_3O_4
		221	3	$Fe_{2+}C$
		168	93	$Fe_{2+}C$

[a] HMF = hyperfine magnetic field.

Table 3
Mössbauer structural analysis for spectra obtained from samples at 20 K for potassium-promoted iron sample

Sample	HMF [a]	Aeral fraction (%)	Phase
3	506	18	Fe_3O_4
	463	16	Fe_3O_4
	256	14	ε-$Fe_2 + C + \chi$-Fe_xC
	185	33	ε-$Fe_2 + C$
	211	11	χ-Fe_xC
	105	8	χ-Fe_xC
5	494	17	Fe_3O_4
	256	10	ε-$Fe_2 + C + \chi$-Fe_xC
	184	60	ε-$Fe_2 + C$
	208	6	χ-Fe_xC
	99	7	χ-Fe_xC
8	494	12	Fe_3O_4
	252	4	ε-$Fe_2 + C$
	184	84	ε-$Fe_2 + C$
11	496	11	Fe_3O_4
	250	3	ε-$Fe_2 + C$
	183	86	ε-$Fe_2 + C$
16	498	8	Fe_3O_4
	250	4	ε-$Fe_2 + C$
	183	88	ε-$Fe_2 + C$

[a] HMF = hyperfine magnetic field.

measurements impact the results primarily by resolving the superparamagnetic identification as Fe_3O_4 and/or iron carbides. In contrast to the unpromoted iron sample which was predominantly the χ-Fe_5C_2 phase, the potassium-promoted sample was predominantly the ε-$Fe_{2+}C$ phase.

The CO conversion with time-on-stream curve for the K-promoted iron catalyst (figure 4) is very similar to the one obtained with the unpromoted iron catalyst. However, while the activity declines with time, the iron carbide phase actually increases with time-on-stream.

3.2. Silicon-promoted iron catalyst

For convenience, this material is referred to as a silicon-promoted iron catalyst although it is realized that Si is most likely present as some form of the oxide and/or carbide. However, efforts to date, using a variety of instrumental techniques, have not produced data that are adequate to define the chemical state of Si in the activated or used samples.

The presence of silicon leads to a significant amount of iron being present in an unknown phase when the measurements were conducted at room temperature (table 4). The measurements that were conducted at low temperature (20 K) for samples 2 and 9 show that the unknown component consists of both Fe_3O_4 and iron carbide. The low-temperature measurements show, to a first approximation, that the amount of each iron phase that is present in the unidentified superparamagnetic form at room temperature is about the same as the distribution of Fe_3O_4 and iron carbide that was obtained with the room temperature measurements of identifiable phases. Only about 50% of the total iron was identified as the iron carbide phases for the room-temperature measurements; however, based on the phases that were identified with the

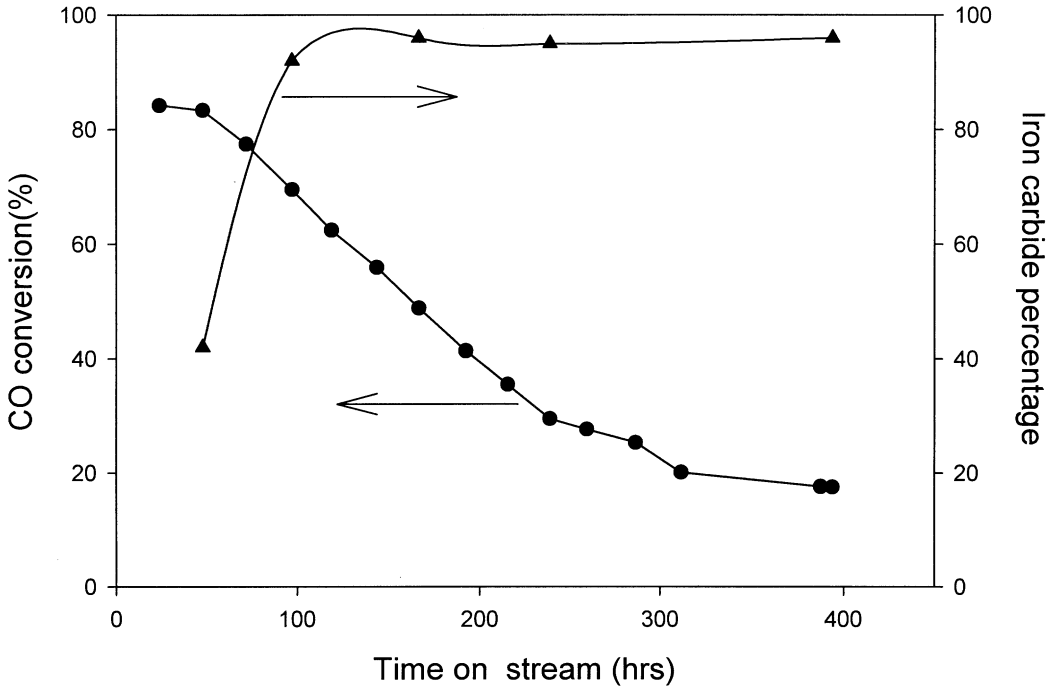

Figure 4. CO conversion and $Fe_{2+}C$ percentage as a function of time-on-stream for the K-promoted iron catalyst.

Table 4
Mössbauer structural analysis for silicon-promoted iron samples

Sample	Time-on-stream (h)	HMF [a]	Atomic aeral fraction (%)	Phase
2 (300 K)	47.8	488	2	A-site Fe_3O_4
		455	6	B-site Fe_3O_4
		213	17	Fe-I in Hägg χ-Fe_3C_2 Carbide
		170	10	Fe-II in Hägg χ-Fe_3C_2 Carbide
		106	11	Fe-III in Hägg χ-Fe_3C_2 Carbide
		Unknown	54	Superparamagnetic
4 (300 K)	94.5	484	2	A-site Fe_3O_4
		455	3	B-site Fe_3O_4
		220	24	Fe-I in Hägg χ-Fe_3C_2 Carbide
		179	21	Fe-II in Hägg χ-Fe_3C_2 Carbide
		107	18	Fe-III in Hägg χ-Fe_3C_2 Carbide
		Unknown	32	Superparamagnetic
7 (300 K)	165.7	485	2	A-site Fe_3O_4
		445	3	B-site Fe_3O_4
		219	20	Fe-I in Hägg χ-Fe_3C_2 Carbide
		177	20	Fe-II in Hägg χ-Fe_3C_2 Carbide
		105	15	Fe-III in Hägg χ-Fe_3C_2 Carbide
		Unknown	40	Superparamagnetic
8 (300 K)	190.8	483	3	A-site Fe_3O_4
		451	9	B-site Fe_3O_4
		220	26	Fe-I in Hägg χ-Fe_3C_2 Carbide
		177	24	Fe-II in Hägg χ-Fe_3C_2 Carbide
		106	16	Fe-III in Hägg χ-Fe_3C_2 Carbide
		Unknown	22	Superparamagnetic
9 (300 K)	215.2	476	2	A-site Fe_3O_4
		453	4	B-site Fe_3O_4
		218	18	Fe-I in Hägg χ-Fe_3C_2 Carbide
		178	19	Fe-II in Hägg χ-Fe_3C_2 Carbide
		102	13	Fe-III in Hägg χ-Fe_3C_2 Carbide
		Unknown	44	Superparamagnetic
2 (20 K)	47.8	504	14	A-site Fe_3O_4
		467	20	B-site Fe_3O_4
		255	30	Fe-I in Hägg χ-Fe_3C_2 Carbide
		208	19	Fe-II in Hägg χ-Fe_3C_2 Carbide
		120	17	Fe-III in Hägg χ-Fe_3C_2 Carbide
9 (20 K)	215.2	504	16	A-site Fe_3O_4
		464	13	B-site Fe_3O_4
		256	30	Fe-I in Hägg χ-Fe_3C_2 Carbide
		205	25	Fe-II in Hägg χ-Fe_3C_2 Carbide
		121	16	Fe-III in Hägg χ-Fe_3C_2 Carbide

[a] HMF = hyperfine magnetic field.

room-temperature measurements, the dominant (>85%) phase was iron carbide (compare spectra in figures 5 and 6). For the low-temperature measurements for samples 2 and 9, taken after about 50 and 215 h of synthesis, the carbide phase represents about 70% of the total iron with the remainder being Fe_3O_4. Furthermore, the fraction of iron carbide, while showing scatter, appears to be nearly constant during more than 250 h of synthesis. Similar to the unpromoted iron catalyst, the dominant iron carbide phase is χ-Fe_3C_2.

The activity of the Si-promoted catalyst is stable for an initial period and then begins to decline (figure 7). However, it does not appear that there is a significant change in the phase composition that follows the loss in activity with time on stream.

3.3. Potassium–silicon-promoted iron catalyst

The phase compositions for the K- and Si-promoted iron catalyst obtained from the low- and high-temperature Mössbauer measurements do not differ significantly with respect to the fraction of carbides except that the fraction is higher by about 10% from the low-temperature measurements (table 5, figure 8). Likewise, apart from sample 9, there is no significant difference in the iron

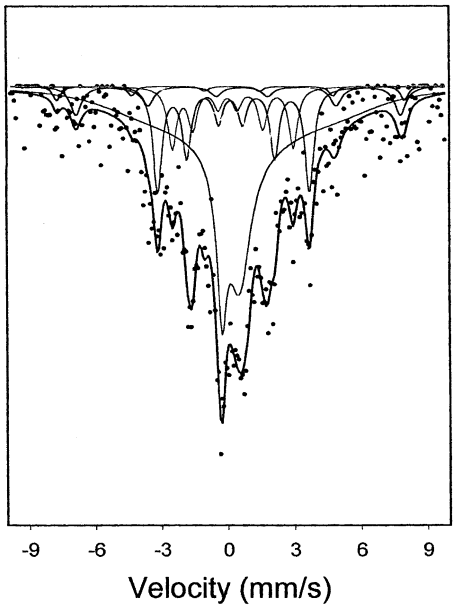

Figure 5. Mössbauer spectrum of Si-promoted catalyst sample (withdrawn at 47.8 hours-on-stream) at room temperature.

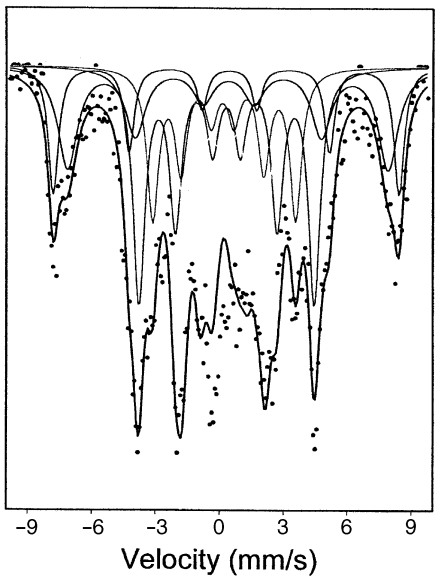

Figure 6. Mössbauer spectrum of Si-promoted catalyst sample (withdrawn at 47.8 hours-on-stream) at 20 K.

phases for the samples withdrawn during the run. Thus, it appears that the doubly-promoted iron catalyst is predominantly present in the iron carbide phase and remains in this phase during the course of the run.

The catalytic activity remained constant during nearly 400 h of the run. This is expected since it has been found repeatedly that the doubly-promoted catalyst that has the same composition is stable for more than five

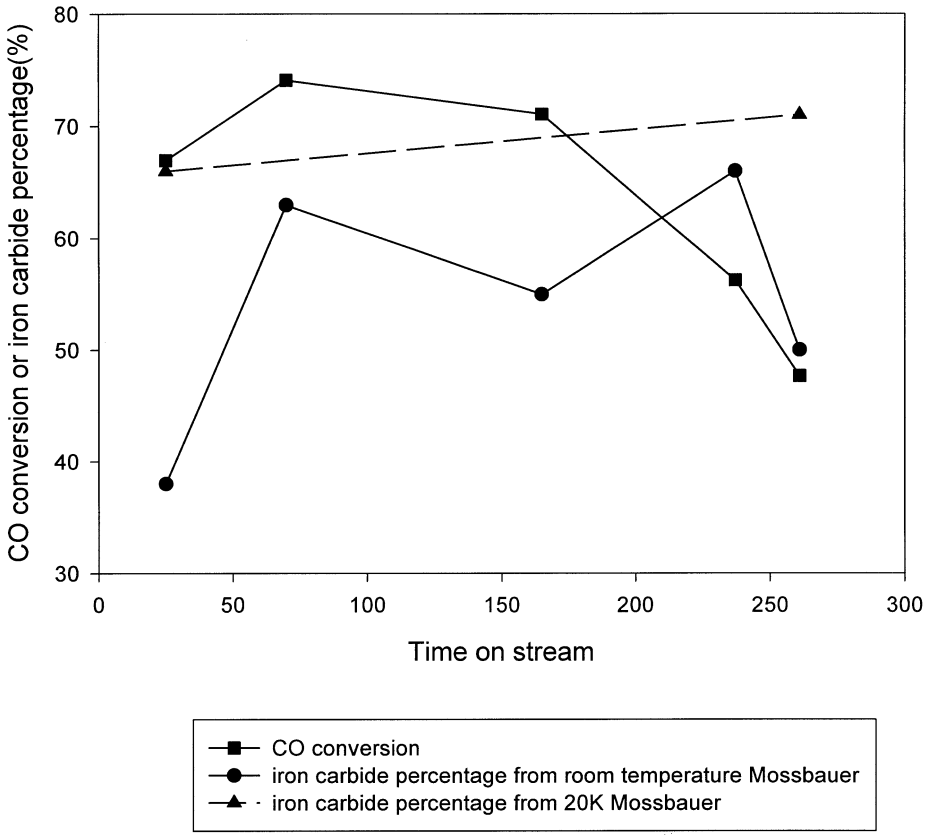

Figure 7. CO conversion and iron carbide percentage *versus* time-on-stream for Si-promoted iron catalyst.

Table 5
Mössbauer structural analysis for potassium–silicon-promoted iron samples

Sample	Time-on-stream (h)	Fraction of iron (%) at 300 K	Phase	Fraction of iron (%) at 20 K	Phase
1	22.9	0	Fe_3O_4	16	Fe_3O_4
		15	$Fe_{2.25}C$	19	$Fe_{2.28}C$
		60	χ-$Fe_{2.34}C$	66	χ-$Fe_{2.30}C$
		24	Superparamagnetic	–	–
4	91.5	3	Fe_3O_4	16	Fe_3O_4
		15	$Fe_{2.25}C$	19	$Fe_{2.28}C$
		65	χ-$Fe_{2.34}C$	66	χ-$Fe_{2.30}C$
		19	Superparamagnetic	–	–
8	187.5	4	Fe_3O_4	16	Fe_3O_4
		16	$Fe_{2.23}C$	16	$Fe_{2.28}C$
		59	χ-$Fe_{2.34}C$	68	χ-$Fe_{2.32}C$
		21	Superparamagnetic	–	–
9	259.5	5	Fe_3O_4	32	Fe_3O_4
		12	$Fe_{2.18}C$	16	$Fe_{2.29}C$
		42	χ-$Fe_{2.39}C$	53	χ-$Fe_{2.32}C$
		40	Superparamagnetic	–	–
13	355.5	7	Fe_3O_4	19	Fe_3O_4
		17	$Fe_{2.22}C$	18	$Fe_{2.25}C$
		50	χ-$Fe_{2.40}C$	63	χ-$Fe_{2.33}C$
		26	Superparamagnetic	–	–

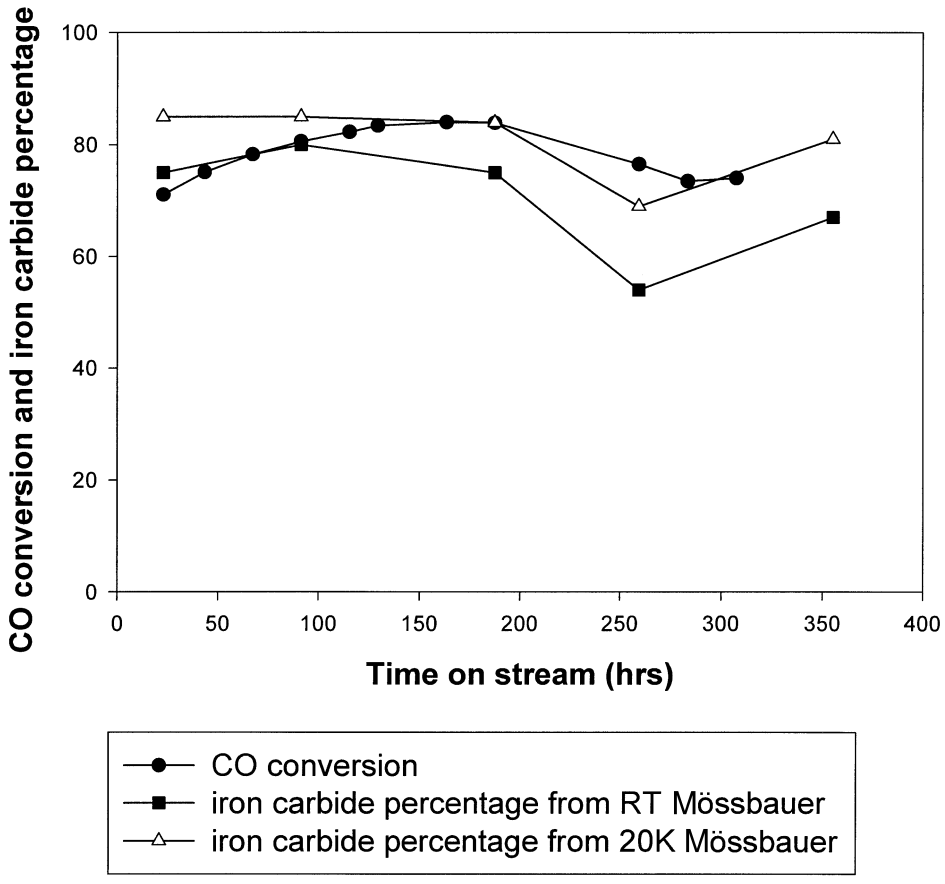

Figure 8. CO conversion and iron carbide percentage from Mössbauer as a function of time-on-stream for the K- and Si-promoted iron catalyst.

months of continuous operation, losing less than 1% of the CO conversion per week [5].

4. Discussion

Based on data generated from several catalysts, a model of the working FT catalyst was developed. In this model, the initial catalyst following activation in CO was essentially a mixture of iron carbides. As the reaction progressed, the carbide fraction decreased to attain a value of about 30–40% [19]. During this phase change, the conversion did not decrease appreciably. To account for the nearly-constant activity while the iron phases changed, a model was proposed. This model had the core of each catalyst particle, initially consisting of an iron carbide phase, oxidizing to form Fe_3O_4 and an outer layer that remains as a carbide form; thus, the surface of the catalyst remained essentially the carbide form while the ratio of oxide/carbide increased as the core consisting of Fe_3O_4 expanded to approach a "steady state" carbide/oxide ratio. The constant conversion while the bulk carbide/oxide ratio changed dictates that the surface composition remain essentially constant throughout the run.

The results with the unpromoted iron catalyst do not agree with this model. Instead, it appears that the catalyst particles convert from the carbide to the oxide form in parallel with the decline in conversion of CO. Thus, it appears that a steady-state particle structure of surface carbide phase/core Fe_3O_4 phase is not formed for the unpromoted iron catalyst. One explanation to account for this is that the rate of iron carbide oxidation is dependent upon the particle size for the unpromoted catalyst or that the oxidation is initiated at the surface and progresses rapidly through the particle compared with FTS.

The results for the potassium-promoted iron catalyst provide a third model for the iron Fischer–Tropsch catalyst as it is used for longer times-on-stream. Initially, the catalyst activity is high and the catalyst is incompletely carbided. As the time-on-stream increases with the unpromoted catalyst, it is oxidized to the Fe_3O_4 phase in parallel with the decline in CO conversion. On the other hand, the potassium-promoted iron catalyst continues to form the iron carbide phase during the initial time-on-stream and the material remains as the carbide phase even though the activity declines with time-on-stream much like the unpromoted iron catalyst. Thus, the presence of potassium maintains the particles as the carbide phase even though it is unable to maintain the catalytic activity.

Intuitively, one might expect that silicon would not impact the formation and/or oxidation of iron carbides; however, this does not appear to be the case. As with the unpromoted iron catalyst, the dominant fraction of the sample is iron carbide after 24 h activation, and the major carbide is χ-Fe_5C_2. Unlike the K-promoted catalyst, the Si-promoted iron catalyst remains as the carbide phase for the duration of the synthesis run while the catalytic activity decreases toward the end of the run. Based upon the X-ray line position, at least some of the Si is incorporated into the lattice of Fe_2O_3 catalyst precursor. It would appear that at least some of the Si must remain incorporated in the bulk of the iron carbide if Si is to impact the stability of the iron carbide during synthesis. One way that it could do this is to remain substituted in the iron carbide lattice and to be present in the working catalyst as silicon carbide; however, this is speculative since no data have been obtained to support this structure. While it is surprising, it seems likely that Si does stabilize iron carbide. Judging from the broad linewidth of the Mössbauer spectra, it appears that at least a part of this stabilization of the carbide phase is due to particle size effects.

Si is usually considered to impact the physical characteristics of the catalyst but not the chemical features. The fraction of ethene in the C_2 fraction is a sensitive measure of the chemical impact of the potassium promoter. Based upon this indicator, Si causes chemical, as well as physical, changes since the ethene fraction is slightly higher for the Si-promoted catalyst than it is for unpromoted iron. Thus, both the Mössbauer and alkene selectivity data indicate that Si can act as a chemical promoter; however, for alkene selectivity it is not nearly as effective as K.

With respect to the K,Si-promoted catalyst, the stable activity and the retention of iron carbide phase was as expected. While earlier runs with similar catalysts showed the stable activity in runs up to more than 3000 h, the amount of carbide in this run is higher than has been obtained in an earlier run [20]. In the earlier run, the amount of iron carbide decreased to about 40% within about 500 h and then remained at this level during the remainder of the run.

These results make it clear that relating the catalyst composition to the catalytic activity of an iron FTS catalyst will be a demanding task. It appears that the carbide phase, or at least a partial carbide phase (iron oxycarbide phase), is more active than the oxide phase. Furthermore, the data for the promoted and unpromoted catalysts show that the initial activity of the χ-Fe_5C_2 phase is as great as the ε- or ε'-carbide (Fe_2C to $Fe_{2.2}C$) phases. The present data do not allow us to decide whether it is the presence of potassium or the stability of the iron carbide phases that allows the ε- or ε'-carbide (Fe_2C to $Fe_{2.2}C$) phases to remain as the conversion declines to a low level while the χ-Fe_5C_2 phase that results for the unpromoted catalyst oxidizes as the conversion decreases. Because the gas present in the reactor becomes more reducing (and to favor carbide formation) as the conversion decreases, it is unexpected for iron oxide to be formed.

It appears that the surface phases are more important than the bulk composition in determining activity and

selectivity. Thus, it appears that it is the relative rate of FTS and the rate of formation of a carbon form that will form a carbide, or oxocarbide, phase in the surface layers that determines that activity level. The data with the unpromoted iron catalyst show that the surface carbide is not formed rapidly enough to maintain a carbide layer thick enough to catalyze FTS at a rapid rate. With the unpromoted catalyst, it appears that the conversion of CO to hydrocarbon products occurs sufficiently rapidly to prevent sufficient carbon being formed to maintain a surface layer or, alternatively, to allow the surface carbon to diffuse into the interior rapidly enough to maintain a surface iron carbide layer sufficiently thick to maintain the high activity. The presence of potassium is not sufficient to maintain catalytic activity but its presence permits the catalyst to produce surface carbon in a form that causes the bulk to remain as the carbide phase. Surprisingly, Si-promotion causes carbon to be produced rapidly enough to maintain a high fraction of the iron in the carbide phase; however, while the Si-promoter imparts catalytic activity for a longer time than the K-promoter, it is a matter of degree rather than long-term activity retention. The Si-promoter does not impact catalytic activity but acts similarly to the K-promoter in maintaining the iron carbide phase and impacting selectivity as the K-promoter does; thus, in these two latter features the Si-promoted catalyst resembles the K-promoted catalyst.

Each of the four catalysts used in this study consists of clusters made up of smaller particles. As the Fe_2O_3 is reduced to Fe_3O_4 and then converted to iron carbides, the bulk X-ray theoretical density decreases to about 50% from the original density. Thus, there is a large increase in the pore volume and the average pore radius as the oxide is converted to the carbide phase. A precipitated iron catalyst was formed into spheres of about 50 μm diameter by spray drying and was carbided using CO in a bubble column reactor. At the end of a 24 h carbiding period, the cluster retained the same average diameter as the as-prepared catalyst, as determined from SEM pictures. Thus, the cluster retained its integrity and original size during carbiding. In a CSTR the cluster is subjected to a much greater stress and will disintegrate into smaller 1–3 μm particles. In both cases the particles consist of iron carbide phases. During use, some fraction of these particles are converted to Fe_3O_4. The model we advanced for the potassium- and silica-promoted catalyst is one where the exterior of the particle retains the carbide phase and the interior is oxidized to Fe_3O_4. This could happen with carbon migrating to the surface to be converted to CO_2 and oxygen migrating into the bulk; however, this is considered to be an unlikely mechanism at these low temperatures. It seems more likely that carbiding and oxidation both occur by diffusion of gaseous reactants rather than migration of atoms or ions through the bulk. The FTS reaction decreases the concentration of both CO and H_2 (both reducing gases) as the reactants diffuse into the catalyst particle (or cluster) and the concentration of H_2O and CO_2 (both oxidizing gases) increases. Under these low-temperature conditions, CO_2 is essentially inert as long as there is competitive adsorption with CO. Water, however, is oxidizing and its high concentration that should be present in the interior of the particle (or cluster) will oxidize the carbide, producing hydrogen and CO_2 and/or CH_4. Thus, the diffusion of gaseous reactants and/or gaseous products will be the vehicle for transport of the species involved in oxidation of iron carbide to Fe_3O_4.

In summary, it appears that the model of the iron FTS catalyst that has a core of Fe_3O_4 surrounded by a surface layer of iron carbides is adequate for the stable, doubly-promoted iron catalyst. However, the retention of the bulk and surface iron carbide phases and bulk carbide are dependent upon the process conditions and the promoters that are present. For normal operating conditions for FTS, the gas-phase composition is one that should produce the iron carbide phases [21]. In the present study, all catalysts exhibit similar conversions at early times on stream and, since they are utilized in a CSTR, will be exposed to similar gas compositions. In this case it cannot be the gas composition that determines the phases of iron that are present. The present results show different behaviors with reaction times that depend upon the promoter present in the catalyst. Thus, the promoter impacts the iron carbide phase that is present during catalyst usage. However, since all four catalysts are more than 80% iron carbides at the start of the FTS, the promoter cannot be the only factor that determines the iron phases present following many hours of use for synthesis. The changes in iron phases and the catalytic activity and selectivities with time show that kinetics of the syngas conversion must impact the catalyst composition. The most reasonable explanation is that the catalytic activity and phase composition are determined by the relative rates of the hydrogenation of surface carbon or carbon-containing species to effect the FTS and the formation of a form of carbon on the surface that is able to diffuse into the bulk to maintain a layer of iron carbide sufficiently thick to produce high catalytic activity. These two rates are apparently balanced with the catalyst containing both K and Si and the catalytic activity is retained during runs of up to six months. This is not the case with the other singly-promoted and unpromoted catalysts. With unpromoted iron, the formation of a surface carbon species is not rapid enough to maintain the carbide phase and catalytic activity is lost. On the other hand, for the potassium-promoted catalyst the surface carbon species forms sufficiently rapidly to maintain the bulk carbide phase but catalytic activity is lost, presumably due to excess surface carbon eliminating sites to adsorb hydrogen.

While the surface composition has not been determined, it has been demonstrated that the catalytic activity is not defined by the bulk phase. By inference, it is concluded that the surface phase, and the ability to retain the optimum phase composition by balancing the rates for FTS and surface carbon concentration, determines the catalytic activity, both initially and with increasing time-on-stream.

Acknowledgments

This work was supported by U.S. DOE contract number DE-FC26-98FT40308 and the Commonwealth of Kentucky.

References

[1] M.E. Dry, in: *Catalysis-Science and Technology* Vol. 1, eds. J.R. Anderson and M. Boudart (Springer, New York, 1981), pp 196–198.
[2] J.P. Reymond, P. Mériaudeau and S.J. Teichner, J. Catal. 75 (1982) 39.
[3] G.B. Raupp and W.N. Delgass, J. Catal. 58 (1979) 361.
[4] C.N. Satterfield, R.T. Hanlon, S.E. Tung, Z. Zou and G.C. Papaefthymiou, Ind. Eng. Chem. Prod. Res. Dev. 25 (1986) 407.
[5] R.J. O'Brien, L. Xu, R.L. Spicer and B.H. Davis, Energy & Fuels 10 (1996) 921.
[6] M.D. Shroff, D.S. Kalakkad, K.E. Coulter, S.D. Köhler, M.S. Harrington, N.B. Jackson, A.G. Sault and A. Datye, J. Catal. 156 (1995) 185.
[7] F.J. Berry and M.R. Smith, J. Chem. Soc. Faraday Trans. 85 (1989) 467.
[8] C.S. Huang, B. Ganguly, G.P. Huffman, F.E. Huggins and B.H. Davis, Fuel Sci. Technol. Int. 11 (1993) 1289.
[9] L. Guczi, Catal. Rev.-Sci. Eng. 23 (1981) 329.
[10] G. Le Caër, J.M. Dubois, M. Pijolat, V. Perrichon and P. Bussiere, J. Phys. Chem. 86 (1982) 4799.
[11] J.A. Amelse, J.B. Butt and L.H. Schwartz, J. Phys. Chem. 82 (1978) 558.
[12] S.A. Eliason and C.H. Bartholomew, *Catalyst Deactivation 1997* eds. C.H. Bartholomew and G.A. Fuentes (Elsevier, Amsterdam, 1997) p. 517.
[13] L.-M. Tau, S. Borcar, D. Bianchi and C.O. Bennett, J. Catal. 87 (1984) 36.
[14] J.W. Niemantsverdriet, A.M. van der Kraan and W.L. van Dijk, J. Phys. Chem. 84 (1980) 3363.
[15] N. Nahon, Thesis, Lyon, 1979.
[16] D. Bianchi, S. Borcar, F. Teule-Gay and C.O. Bennett, J. Catal. 82 (1983) 442.
[17] R.R. Gatte and J. Phillips, J. Catal. 104 (1987) 365.
[18] A. Raje, R.J. O'Brien, L. Xu and B.H. Davis, *Catalyst Deactivation 1997*, *Studies in Surface Science Catalysis*, eds. C.H. Bartholomew and G.A. Fuentes, 111 (1997) 527.
[19] B.H. Davis, *Technology Development for Iron Fischer–Tropsch Catalysis*, DOE contract DE-AC22-94PC94055, Final Report, March, 1999.
[20] N.B. Jackson, A.K. Datye, L. Mansker, R.J. O'Brien and B.H. Davis, in *Catalyst Deactivation 1997*, *Studies in Surface Science Catalysis*, eds. C.H. Bartholomew and G.A. Fuentes, 111 (1997) 501.
[21] S.J. Liaw and B.H. Davis, Topics Catal. 10 (2000) 133.